Model-based prognosis of fatigue crack growth under variable amplitude loading

Elinirina Robinson, Julien Marzat, Tarek Raïssi

Model-based prognosis of fatigue crack growth under variable amplitude loading

Elinirina I. Robinson * **Julien Marzat** * **Tarek Raïssi** **

* *DTIS, ONERA, Université Paris-Saclay, F-91123 Palaiseau, France (e-mail: elinirina.robinson@onera.fr, julien.marzat@onera.fr).*
** *CEDRIC-Lab, Conservatoire National des Arts et Metiers, Paris 75141, France (e-mail: tarek.raissi@cnam.fr).*

Abstract: In this paper, a model-based prognosis method using a particle filter that takes model uncertainty, measurement uncertainty and future loading uncertainty into account is proposed. A nonlinear analytical model of the degradation that depends on loading parameters is established, and then a particle filter is used to estimate and forecast these unknown inputs at the same time as the degradation state. Moreover, adding to this joint input-state estimation, a two-sided CUSUM algorithm is implemented to detect load variations. This would help the prognosis module to adapt to a change in the degradation state evolution, in order to correct the remaining useful life prediction. Real data from fatigue tests on fiber-reinforced metal matrix composite materials are used to demonstrate the efficiency of the proposed methodology for crack growth prognosis.

Keywords: Model-based prognosis, unknown inputs estimation, particle filter, uncertainty propagation, fatigue crack growth, composite materials.

1. INTRODUCTION

Failure prognosis aims at calculating the remaining useful life (RUL) of a system, which is the time available until the monitored system no longer behaves properly. Because of economic and human safety challenges, the prediction of the RUL must be as reliable as possible to allow risk-based decisions. For this purpose, prognosis methods should account for the different uncertainty sources that affect the estimation of the current and future health state of the system, and thus provide a measure of the uncertainty affecting the predicted RUL (Tang et al., 2009; Baraldi et al., 2013). The main types of uncertainty that inevitably influence RUL prediction are measurement uncertainty, modeling uncertainty and future loading uncertainty (Gu et al., 2007). Measurement uncertainty is due to sensor inaccuracy, modeling uncertainty is characterized by the difference between the crack growth model and its real behavior, and future loading uncertainty is caused by various environmental factors that could possibly affect the evolution of the crack length. In order to correctly deal with these uncertainties, appropriate uncertainty representation and propagation methods must be chosen (Orchard et al., 2008).

In the literature, various model-based crack growth prognosis methods using a probabilistic approach for uncertainty representation and propagation have been developed (Saha and Goebel, 2008). For instance, (Corbetta et al., 2015) proposed a particle filter sequentially updated via a Metropolis-Hastings (MH) algorithm for crack growth prognosis on helicopter fuselage panels. A machine learning approach based on artificial neural networks was used to estimate the stress intensity factor (SIF) range, which is required to calculate the crack growth at each cycle. In (Zárate et al., 2012), the SIF range was modeled by a polynomial equation with stochastic coefficients that were computed through Bayesian inference. The future crack length was then predicted using a Markov Chain Monte Carlo algorithm. The ability of these methods to predict the RUL of components subject to fatigue crack growth under measurement and modeling uncertainty has been proved through numerical examples. However, they have assumed known values of the current and future loading, which is not the case in real life scenario.

In order to address this issue related to the estimation of the loading amplitude, other researchers have introduced crack growth prognosis methods based on structural health monitoring data. The main idea is to use real-time monitoring data to build models that characterize fatigue loading history, and then based on these models, the future loading can be predicted. In (Ling and Mahadevan, 2012), both flight parameters data related to acceleration and mass and data recorded from strain gauges were used to estimate and predict loading sequence through an autoregressive integrated moving average (ARIMA) modeling method and a Bayesian approach for the update process. The evaluation of the SIF range required for the crack growth calculation was made with a Gaussian process surrogate model that was previously trained with data from a finite element analysis. In (Pais and Kim, 2015), usage monitoring data from an aircraft (acceleration, airspeed, angle of attack, fuel quantity and Mach number) were converted into a stress time history which was then transformed into a cyclic stress history via a rain-flow counting algorithm. The resulting cyclic stress history was used to consider the effects of variable amplitude loading in the determination of the crack growth direction. However,

it was suggested that it could be used as the input into a prognosis method. What these proposed methodologies have in common is that real-time monitoring data related to the loading or flight parameters are required to build a model that characterizes the stress history. Moreover, a finite element model was needed for the calculation of the SIF range or to train its surrogate model.

In this paper, it is assumed that only crack length measurements are available, and no finite element model is used. Indeed, the effort was focused on the derivation of an analytical model of the SIF range, which contains parameters that are directly related to the applied load. It was then decided to perform the joint estimation of the crack length and of the unknown loading parameters through the use of a particle filter. The ability of the particle filter to perform uncertainty propagation but also to deal with the high nonlinearities of the SIF range analytical model has motivated this choice. Moreover, as the particle filter is a Bayesian filter method, the RUL predictions are improved as new crack length data are collected.

The article is organized as follows. Section 2 gives information about the composite material that was used to collect the data, and then a detailed description of the crack propagation model is provided. In Section 3, the joint input-state estimation methodology with the particle filter is presented, as well as the two-sided CUSUM algorithm. Then, numerical results which illustrate the efficiency of the prognosis method on real fatigue crack growth data are reported in Section 4. Finally, a general conclusion about the proposed prognosis methodology and perspectives for future work are summed up in Section 5.

2. PROBLEM STATEMENT

In this section, a model to assess dynamic crack propagation in fiber-reinforced metal matrix composites is presented. Before introducing this model, the experimental procedure to collect the real crack growth data used in this work is described.

2.1 Material and experimental procedures

A composite material is the combination of two or more different materials in order to create a superior material with different properties (stronger, lighter, ...). Composites are mainly made up of two constituent materials: matrix and reinforcement. There are three main kinds of materials that are used for the matrix (polymer, metal and ceramic) and also different kind of forms for the reinforcement material (particles, fibers or laminates). In this work, the proposed methodology is applied to fatigue crack growth prognosis in titanium metal matrix composites with silicon carbide fibers used as reinforcement materials. The fatigue test data were previously used in (Maire et al., 2000) to establish and validate a model to describe the fatigue crack growth in the concerned specimens, but the problem of RUL prognosis was not addressed. For consistency, the experimental protocol is summarized in what follows.

The titanium-matrix composite studied was SCS-6/Ti-6242. Ti-6242 is a near alpha titanium alloy with the composition Ti-6Al-2Sn-4ZR-2Mo (percent by weight), and this matrix was reinforced with 140 μm diameter SCS-6 Textron fibers. The fibers are regularly spaced in the matrix in such a way as to obtain a unidirectional composite. A parallelepiped notched specimen (Fig. 1) with a nominal width of 8 mm, thickness of 2.1 mm and length of 160 mm was machined from the composite material in a manner that the length of the specimen is parallel to fiber axis. The elliptic notch of 0.75 mm length is located in the middle of the specimen.

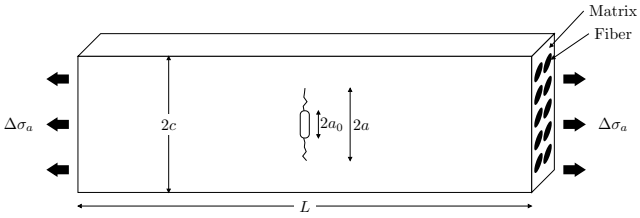

Fig. 1. Schematic of the specimen showing the dimensions and the loading axis parallel to fiber direction

The crack length data that are used in this work are from a specimen that was tested under variable amplitude loading. The cyclic loading was uniaxial and oriented along the fiber direction. The stress ratio $R = \sigma_{min}/\sigma_{max}$ was equal to 0.1. The fatigue tests were performed at room temperature and at 400°C under a frequency of 50 Hz. In order to measure the crack length, photographs of the crack extension were recorded by a digital camera monitored by a computer. The typical cracking geometry involved the propagation of a crack in the matrix on each side of the notch, propagating perpendicularly to the loading direction.

The crack propagated through all the thickness of the specimen and across its entire width without causing the rupture of the composite material. This phenomena is due to unbroken fibers that have bridged the matrix crack. Indeed, as the fiber stress level did not exceed the value of the fiber strength, no fiber broke during the experiments. The constraints of these bridging fibers can be modeled by the distribution of a closure pressure $P(x)$ acting in the direction opposite to the applied stress σ_a in the bridged zone (Fig. 2). In this case, the bridged zone is equivalent to the crack length minus the notch length $2a_0$.

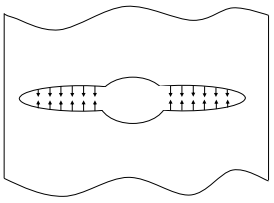

Fig. 2. The closure pressure in the crack wake

2.2 Description of the crack propagation model

It is assumed that the composite has a linear elastic behavior except in a very small region at the crack tip, therefore the principles of linear elastic fracture mechanics can be applied. The following modified Paris' law that was previously used in (Maire et al., 2000) to study the same fatigue test dataset can then be used to model the Mode I crack propagation:

$$\frac{da}{dN} = C(\Delta K_m - K_{th})^m \tag{1}$$

where a is the crack size, N is the number of cycles. Since the crack growth observed in the composite material was limited to the matrix cracking, the effective crack-driving force is assumed to be the SIF range ΔK_m experienced by the matrix. The constants C, m and K_{th} depend on matrix properties. K_{th} is the threshold value of the SIF below which no crack growth occurs.

The calculation of the SIF range ΔK_m is the main challenge in this modeling stage. A simple expression of the SIF range can be available. However, in more complex structures as composite materials, an analytical closed form of the SIF does not always exist or is too complicated to establish. In these cases, finite element simulations can be run to calculate the SIF values associated to different crack lengths. Then, based on the obtained database of SIFs, a regression model is used to allow the evaluation of the SIF for any crack length. This technique was used in (Corbetta et al., 2015) where a machine learning approach based on artificial neural networks was used to provide estimates of SIFs. In (Neerukatti et al., 2014), two regression techniques were used, namely least absolute shrinkage and selection operator (LASSO) and relevance vector machine. Although very efficient to obtain good estimations of the SIF, the main drawback of such an approach is the high computational time induced. In this work, an analytical expression of the stress intensity factor for bridged cracks in composite materials was established, based on different studies found in (Johnson et al., 1996).

The first step to determine ΔK_m is to relate it to the continuum SIF range ΔK_{tip} which is the homogenized composite stress intensity factor. Many discrete-continuum relationships were proposed, and three of them were compared in (Bakuckas and Johnson, 1993). In their study, the one that gave the best results in the modeling of fiber-bridging effect on ΔK_m was established by (McMeeking and Evans, 1990):

$$\Delta K_m = \Delta K_{tip} \tag{2}$$

In order to calculate ΔK_{tip}, the weight function technique proposed by (Bueckner, 1970) that allows to calculate a stress intensity factor for arbitrary stress distributions is applied. In this case study, the applied stress range on the crack surface is $\Delta\sigma_{br} = \Delta\sigma_a - \Delta P(x)$, therefore we have:

$$\Delta K_{tip} = 2\int_0^a (\Delta\sigma_a - \Delta P(x))G(x,a,c)\mathrm{d}x \tag{3}$$

where $G(x,a,w)$ is a weight function that depends on the geometry of the specimen, c is the specimen width and $2a$ is the crack length.

For a center crack configuration in a finite width specimen, the following expression of ΔK_{tip} is finally obtained (Zheng and Ghonem, 1996):

$$\Delta K_{tip} = F\Delta\sigma_a\sqrt{\pi a} - 2F\sqrt{\frac{a}{\pi}}\int_{a_0}^a \frac{\Delta P(x)}{\sqrt{a^2-x^2}}\mathrm{d}x \tag{4}$$

where F is a geometric factor that depends on the specimen width (various expressions can be found in (Tada et al., 1973)), $2a_0$ is the length of the unbridged zone (i.e. notch length) and x is the distance from the crack center. It can be noticed that this expression of ΔK_{tip} takes into account both the contribution of the applied remote stress $\Delta\sigma_a$ and the contribution of the bridging stress $\Delta\sigma_{br}$ produced by unbroken fibers in the crack wake.

Finally, the model that describes crack growth propagation in the studied specimens is given by:

$$\frac{da}{dN} = C\left(F\Delta\sigma_a\sqrt{\pi a} - 2F\sqrt{\frac{a}{\pi}}\int_{a_0}^a \frac{\Delta P(x)}{\sqrt{a^2-x^2}}\mathrm{d}x - K_{th}\right)^m \tag{5}$$

The determination of the change in closure pressure $\Delta P(x)$ is the critical issue of the fatigue crack propagation problem in fiber reinforced composites. In the literature, two types of analytical models have been widely used to calculate $\Delta P(x)$: (i) the shear-lag model and (ii) the fiber pressure model. For more details about these two approaches, the reader may refer to (Ghosn et al., 1992). As an alternative to these methods, (Davidson, 1992) has used a uniform closure pressure over the entire bridged zone and obtained satisfying results for SCS-6/Ti-6Al-4V composite materials. This approach was considered in this paper as it allows to avoid the integration of $P(x)$ to calculate ΔK_{tip}, which highly decreases the computational time. Indeed, this is an important criteria for online RUL prognosis.

Adopting this constant approximation of the closure pressure leads to the following model:

$$\frac{da}{dN} = C\left(F\Delta\sigma_a\sqrt{\pi a} - 2F\sqrt{\frac{a}{\pi}}\Delta P\int_{a_0}^a \frac{1}{\sqrt{a^2-x^2}}\mathrm{d}x - K_{th}\right)^m \tag{6}$$

where

$$\int_{a_0}^a \frac{1}{\sqrt{a^2-x^2}}\mathrm{d}x = \frac{\pi}{2} - \arcsin\left(\frac{a_0}{a}\right). \tag{7}$$

Finally, the model that is used for crack growth prognosis in the studied fiber-reinforced titanium matrix composite material is:

$$\frac{da}{dN} = C\left(F\Delta\sigma_a\sqrt{\pi a} - 2F\sqrt{\frac{a}{\pi}}\Delta P\left(\frac{\pi}{2} - \arcsin\left(\frac{a_0}{a}\right)\right) - K_{th}\right)^m \tag{8}$$

The model (8) that was obtained contains two terms that are directly related to the applied load, namely $\Delta\sigma_a$ and ΔP. Therefore, a joint input-state estimation will allow the constant monitoring of external loads while estimating the crack length. A particle filter is used in this study not only because of its ability to perform this joint estimation but also to deal with uncertainty propagation and high nonlineartities.

3. PARTICLE FILTER AND TWO-SIDED CUSUM ALGORITHMS FOR JOINT INPUT-STATE ESTIMATION

In the proposed methodology for model-based prognosis in presence of unknown loading inputs, a particle filter for joint input-state estimation is combined with a two-sided

CUSUM algorithm. The idea is to jointly estimate the degradation state along with the unknown loading inputs with the particle filter, while monitoring the estimation of the inputs with the two-sided CUSUM algorithm to detect load variations. In the case where a load variation is detected, the CUSUM algorithm informs the particle filter which has then to reinitialize the loading inputs values in order to improve the quality of RUL predictions after load variation.

In this section, the sequential importance resampling (SIR) particle filter is first introduced, then the two-sided CUSUM algorithm is presented, and finally model-based prognosis process under unknown loading inputs that uses the combination of these two techniques is described.

3.1 Particle filter for joint input-state estimation

Particle filter allows to recursively calculate and update the probability density function (pdf) of a state vector x_k based on the following discrete state-space system:

$$x_k = f(x_{k-1}, u_{k-1}, w_k) \tag{9}$$
$$y_k = h(x_k, v_k) \tag{10}$$

where $x \in \mathbb{R}^n$ denotes the state, $u \in \mathbb{R}^m$ represents the inputs vector, $y \in \mathbb{R}^p$ is the measured outputs and $k \in \mathbb{N}$ is a discrete time step. The functions f and h describe respectively the nonlinear evolution of the state and the measurements over time. The variables w and v are respectively the process and measurement noises.

In this work, the unknown loading inputs denoted by the vector $u \in \mathbb{R}^m$ are included in the state vector $x \in \mathbb{R}^n$. This allows to form an augmented state vector $X = [x\ u]$ in order to perform the identification of the unknown inputs in conjunction with state estimation using the particle filter.

In the particle filter approach, the state pdf at time instant k is approximated by a set of N_{part} particles $\{X_k^i\}_{i=1}^{N_{part}}$ representing points in the state space, and a set of associated weights $\{\omega_k^i\}_{i=1}^{N_{part}}$ denoting discrete probability masses:

$$p(X_k|y_{0:k}) \approx \sum_{i=1}^{N_{part}} \omega_k^i \delta(X_k - X_k^i) \text{ with } \sum_{i=1}^{N_{part}} \omega_k^i = 1 \tag{11}$$

where δ is the Dirac delta function.

There exist several PF algorithms (Arulampalam et al., 2002). One of the most used is the sequential importance resampling (SIR) particle filter. It is based on three main steps that are prediction, update and re-sampling:

(1) Initialization
- Draw particles $X_0^i \sim p(X_0)$
- Compute the initial weights $\omega_k^i = \frac{1}{N_{part}}$

Prediction
- Simulate the state equation (9) to generate a new set of N_p particles $X_k^{i=1:N_{part}}$ which are realizations of the predicted pdf $p(X_k|y_{0:k-1})$.

(2) Update
- Each sampled particle is assigned a weight based on the likelihood $p(y_k|X_k)$:

$$\omega_k^i = \omega_{k-1}^i p(y_k|X_{k-1}^i) = \omega_{k-1}^i \frac{p(y_k|X_k^i)p(X_k^i|X_{k-1}^i)}{p(X_k^i|X_{k-1}^i, y_k)} \tag{12}$$

- Normalize the weights:

$$\omega_k^i = \omega_k^i \left(\sum_{i=1}^{N_{part}} \omega_k^i \right)^{-1} \tag{13}$$

(3) Re-sampling
- Degeneracy problem: the weight variance increases and after a few iterations all but one particle may have a negligible weight (Daum, 2005). Particles with small weights are eliminated so that the computational efforts are concentrated in those having large ones.
- Re-sampling condition: if the effective sample size N_{eff} is under some threshold N_{th}, a re-sampling procedure is done. An estimate of N_{eff} is

$$\hat{N}_{eff} = \left(\sum_{i=1}^{N_{part}} (\omega_k^i)^2 \right)^{-1} \tag{14}$$

- Using the inverse cumulative distribution function method (Arulampalam et al., 2002) and the current set $\{X_k\}_{i=1}^{N_{part}}$, a new set $\{\tilde{X}_k\}_{i=1}^{N_{part}}$ is drawn to replace the current one. Finally, with $\tilde{\omega}_k^i = N_{part}^{-1}$, the state is given by:

$$\hat{X}_k^i = \sum_{i=1}^{N_{part}} \tilde{\omega}_k^i \tilde{X}_k^{\ i} \tag{15}$$

This basic SIR particle filter algorithm is applied during the first step of the prognosis process which consists in estimating the current augmented state vector using data from the different sensors. This step is realized as long as measurements are available until the prediction time k_p from which a prediction of the future augmented state vector is performed. During the forecasting step, no more measurements are collected. However, the update of the particle weights depends on the acquisition of new measurements. To overcome this difficulty, the state is propagated only using the state model (9) while the particle weights are propagated in time without any changes. In other words, only the prediction step is repeated until the chosen failure threshold is reached. Considering that the particle weights are invariant for time instants $k > k_p$ leads to a negligible approximation error with respect to other sources of error such as wrong choices of noise parameters or model inaccuracies (Orchard and Vachtsevanos, 2007).

The efficiency of this particle filter algorithm has already been proved for joint state and model parameters estimation in (Robinson et al., 2016). However, in this paper, the main challenge concerns the estimation of the unknown inputs, whose initial values have to be set for the initialization step of the particle filter algorithm. As there is an uncertainty related to this value, it is proposed to consider that it is included in an interval $I_0 = [\underline{I_0}, \overline{I_0}]$. It is demonstrated in Section 4 that this assumption holds as the proposed particle filter has the ability to readjust the estimation thanks to the model and to the measurements.

3.2 Two-sided CUSUM algorithm

A basic two-sided CUSUM algorithm is used for the detection. It is the combination of two CUSUM algorithms,

where one is for the detection of an increase in the mean of the monitored variable, and the other one to detect a decrease in the mean. The general idea is to calculate a cumulative sum S_k that depends on the monitored process Δx, on its initial mean value μ_0 and on the minimal size of change to detect denoted by ν. And when the value of the sum exceeds a defined threshold value S_{th}, a change in the mean value is detected. Therefore, the two-sided CUSUM algorithm is based on the following equations:

$$\begin{cases} S_k^+ & = \max\left(0, S_{k-1}^+ + \Delta x_k - \mu_0 - \frac{\nu}{2}\right) \\ S_k^- & = \max\left(0, S_{k-1}^- - \Delta x_k - \mu_0 - \frac{\nu}{2}\right) \\ N_{detect} & = min\{k : S_k^+ \geq S_{th} \cup S_k^- \geq S_{th}\} \end{cases} \tag{16}$$

where N_{detect} is the time at which the detection is made. There are two parameters that have to be chosen in this algorithm: S_{th} and ν. This choice depends on how the signal to process looks like, and for a Gaussian distribution, one can set $S_{th} = 2\frac{\sigma_{\Delta x}}{\nu}$ where $\sigma_{\Delta x}$ is the standard deviation of Δx. Further information about the two-sided CUSUM algorithm can be found in (Blanke et al., 2006).

3.3 Prognosis methodology with the particle filter and the detection algorithm

The constant monitoring of inputs with the detection algorithm allows not only to detect abrupt load variations but also to reinitialize the input value right after the alarm. This would help the particle filter to converge more quickly and more easily to the actual degradation state. This procedure leads to the introduction of a new uncertain parameter which is the initial loading input value after load variation. In most cases this value is unknown, but the user may have an order of magnitude of it. Indeed, depending on the monitored system, the critical input value that can accelerate the degradation state evolution can be obtained from expert knowledge. Therefore, because of the uncertainty associated to this value, it is included in an interval $I = [\underline{I}, \overline{I}]$ as it was the case for the initial input value at the beginning of the particle filter algorithm.

An illustration example is given in the next section in order to have a better comprehension and to quantify the efficiency of the proposed methodology for model-based prognosis.

4. NUMERICAL RESULTS

In this section, the results of the application of the proposed methodology for model-based fatigue crack growth prognosis are provided. Real data from fatigue tests on the fiber-reinforced composite material presented in Section 2 is used.

4.1 Initialization of the prognosis algorithm

For the study, the following discrete-time form of the crack growth model (8) is used:

$$a_{k+1} = a_k + C\Delta N \left[F\Delta\sigma_{a_k}\sqrt{\pi a_k} - 2F\sqrt{\frac{a}{\pi}}\Delta P_k\left(\frac{\pi}{2} - \arcsin\left(\frac{a_0}{a_k}\right)\right) - K_{th}\right]^m \tag{17}$$

This model is randomized in order to take the different uncertainty sources into account. Modeling and measurement uncertainty are integrated by adding zero-mean Gaussian noises to the state and measurement equations, that are respectively w_k and v_k. Moreover, the unknown loading parameters $\Delta\sigma_{a_k}$ and ΔP_k are considered as random variables. The variances of all these stochastic variables that were used for the implementation of the particle filter algorithm are listed in Table 1.

Table 1. Distributions of random parameters

Parameter	$\Delta\sigma_a$	ΔP	w	v
Variance	5×10^{-3}	5×10^{-3}	10^{-6}	6×10^{-3}

The objective here is to jointly estimate and forecast the crack length and the two unknown loading parameters, therefore the augmented state vector is defined as $x_k^\top = [a_k \ \Delta\sigma_{a_k} \ \Delta P_k]$.

The values of the initial state vector have to be determined for the initialization of the particle filter algorithm. The initial crack length a_0 is supposed to be known because the prognosis module is launched only if a crack growth is detected in the monitored component. In the tested specimen, this value is $a_0 = 0.7$mm. Concerning the inputs loading parameters $\Delta\sigma_a$ and ΔP, their initial values are assumed to be included in the interval $I_0 = [300, 400]$.

In this work, the material parameters m and C are assumed to be constant variables as the focus is placed on the estimation of the unknown inputs related to loading amplitude. They have already been calculated in a previous work, and we have $m = 2.4$ and $C = 5.4 \times 10^{-11}$. Finally, a total number of 500 particles was used by the filter. In the figures that will be presented in the next subsections, the plotted curves correspond to the mean estimation.

4.2 Fatigue crack growth under constant amplitude loading

In this subsection, the case of fatigue crack growth under constant amplitude loading is treated.

The first step of prognosis consists in jointly estimating the current crack length a and the unknown inputs $\Delta\sigma_a$ and ΔP using the crack growth model and the collected crack length data at each time step k corresponding to a cycle number N. Then, from a prediction time cycle N_p, the forecasting of the future state vector is performed without any measurements.

First of all, in order to demonstrate the robustness of the proposed particle filter to the initial unknown loading inputs values, the prognosis results for different initial values of $\Delta\sigma_a$ and ΔP in I_0 have been plotted in Fig. 3.

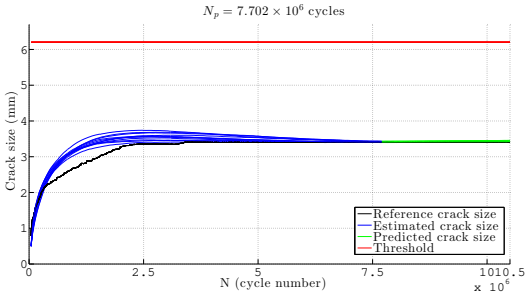

Fig. 3. Crack length evolution with $N_p = 7.702 \times 10^6$ cycles

It can be seen that despite the uncertainty in the initial loading input values, the particle filter always manages to converge to the actual crack length. This is an important feature of the proposed joint input-state estimation algorithm because in real-time prognosis, this value is unknown.

Moreover, one can notice that the crack length does not increase and the estimated unknown loading parameters remain constant after the transient state (Fig. 4). Indeed, as the tested specimen was under plane stress, the crack will stop growing if the applied load is kept constant. Therefore, the crack growth reaches a steady-state and the failure threshold will not be reached.

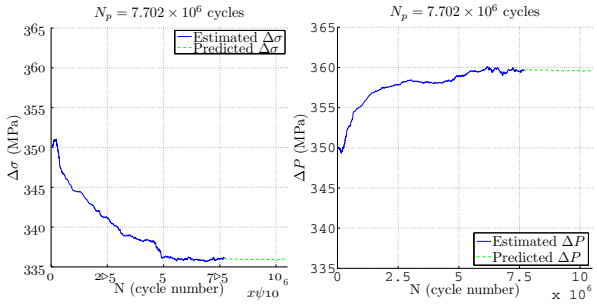

Fig. 4. Crack length evolution with $N_p = 7.702 \times 10^6$ cycles

In the next subsection, a case of crack growth under variable amplitude loading is treated to prove the ability of the proposed methodology to jointly estimate the crack length and the unknown loading parameters even in these circumstances.

4.3 Fatigue crack growth under variable amplitude loading

In this subsection, crack growth prognosis under variable amplitude loading is considered. The crack length measurements are from the real dataset obtained during fatigue test on fiber-reinforced titanium matrix composite materials presented in Section 2.

As a first step, the estimation of the crack length and the unknown loading parameters is performed using the available measurements. Then, the forecasting step is realized from the prediction time cycle N_p. Before load variation, the prognosis results are the same as described in the previous subsection. After load variation, the forecasting of the future crack growth without new measurements is made at different prediction time cycles N_p. The evolution of the future crack length predictions are depicted in Fig. 5. The first part of the crack length evolution is not shown as it is the same as in Fig. 3.

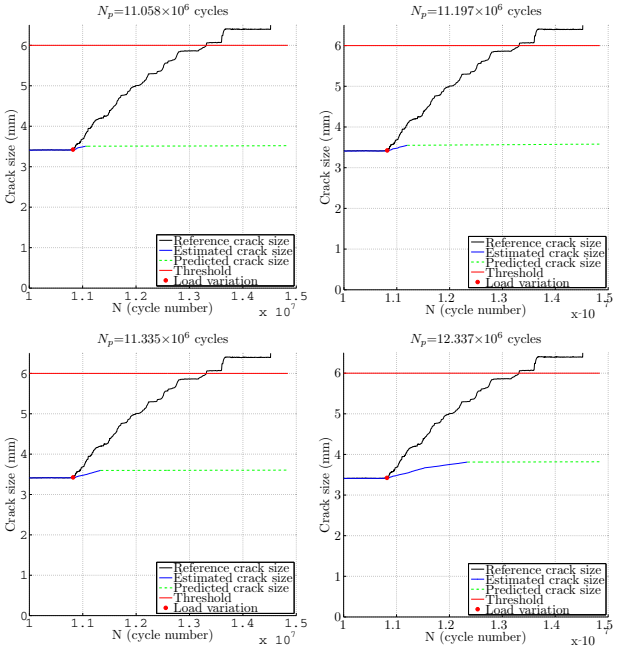

Fig. 5. Evolution of the crack length at different prediction cycles N_p

The higher amplitude of the external applied load has led to an increase in the crack length, which indicates that the critical stress has been attained. The results show that the particle filter has some difficulties to converge even after several time cycles of estimation using the measurements. Indeed, the particle filter needs more data in order to estimate the unknown loading parameters whose values have significantly increased after this abrupt load variation. This problem could be addressed by increasing the number of particles. In this study, 500 particles were used, and a test with 3000 particles was realized. The results were almost the same, and this number cannot be further increased because the computational time would be too important, which is not suitable for online applications.

In order to circumvent this issue, the two-sided CUSUM algorithm presented in Section 3 is integrated to the particle filter. The estimated values of the unknown loading inputs $\Delta\sigma_a$ and ΔP are constantly monitored to detect the sudden load variation. Indeed, as these inputs are related to the applied load, when the loading amplitude changes, their values change as well (Fig. 6). It can be seen that this monitoring must start after the transient state to avoid any false detection. The minimal size of change to detect in the unknown inputs variables was fixed to $\nu = 2$ MPa. The two-sided CUSUM algorithm has detected the variation at $N_{detect} = 10.881 \times 10^6$ cycles while the actual load variation time is $N_{load} = 10.868 \times 10^6$ cycles.

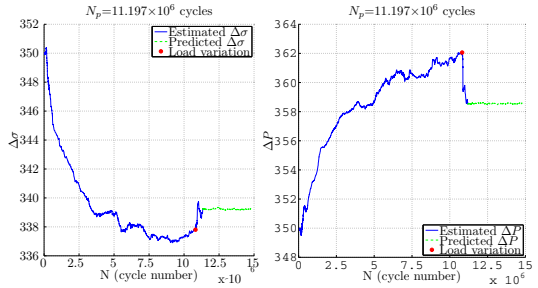

Fig. 6. Abrupt change in $\Delta\sigma_a$ and ΔP after load variation

After the detection of load variation, the values of $\Delta\sigma_a$ and ΔP are reinitialized. The choice of the interval I is based on the a priori knowledge of the necessary load amplitude that may cause a rapid propagation of the crack in the considered specimen. The values $\Delta\sigma_{a_{crit}}$ and ΔP_{crit} associated to the critical load are known to be around 450 MPa. Therefore, in order to take the uncertainty associated to this value into account, it was considered that the reinitialized values of $\Delta\sigma_a$ and ΔP belong to the interval $I = [400, 500]$. This has allowed to estimate and then forecast an interval that contains the crack length after load variation. The bounds of this interval are derived from two extreme loading cases. The evolution of this confidence interval for different prediction cycles N_p is shown in Fig. 7.

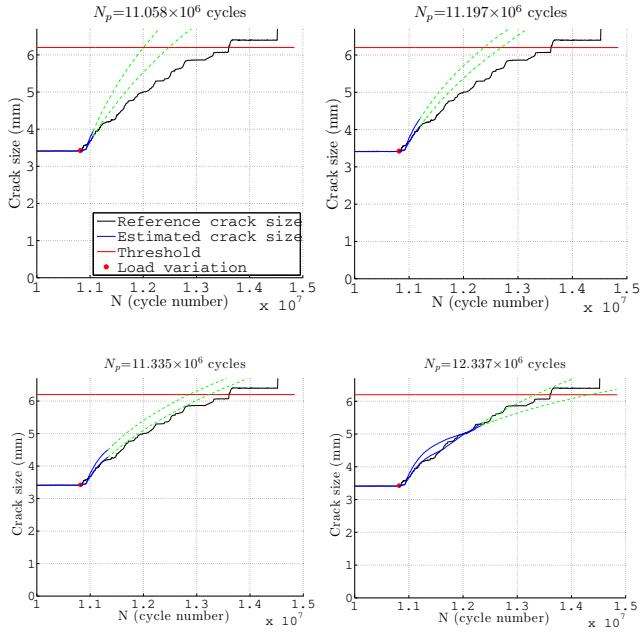

Fig. 7. Evolution of the crack length at different prediction cycles N_p with the detection algorithm

First of all, the gain of the detection algorithm and the reinitialization of the inputs values is highlighted in these figures. It can be seen that even if the input values after the load variation are uncertain, the confidence interval that was derived from the interval I in which the reinitialized values of $\Delta\sigma_a$ and ΔP are included still give an accurate prediction of the future crack length. Moreover, the predictions improve as more data is available. Even if the plotted results give an idea about the efficiency of the proposed methodology, a more precise performance evaluation using metrics such as accuracy, precision and timeliness has been performed.

Accuracy measures the degree of closeness of the predicted RUL to the actual RUL, and its values are between 0 and 1 where 1 gives the best accuracy. Precision evaluates the narrowness of the interval in which the RUL predictions fall, and ranges between 0 and 1 which reflects the highest precision. Finally, timeliness indicates the relative position of the predicted RUL pdf along the time axis with respect to the occurrence of the actual failure event. There are three cases: (i) the failure occurs after the predicted failure time, (ii) the failure occurs at the same time as the predicted failure time, and finally, (iii) the failure occurs earlier than predicted. This last case must be absolutely avoided, that is why the timeliness function allows to penalize late predictions. Timeliness has positive values and 0 is the best score. More details about the formulation of these metrics can be found in (Robinson et al., 2016).

The metrics were calculated for several reinitialization values of $\Delta\sigma_a$ and ΔP included in I. Indeed, it allows to take the uncertainty related to these values into account. The mean values and the standard deviation of each metrics in the predicted confidence interval are given in Table 2.

Table 2. Performance evaluation results

Prediction time	Accuracy	Precision	Timeliness
11.058×10^6	0.59 (±0.04)	0.62 (±0.02)	4.56 (±1.05)
11.197×10^6	0.65 (±0.04)	0.75 (±0.02)	2.74 (±0.73)
11.335×10^6	0.81 (±0.08)	0.86 (±0.04)	0.92 (±0.46)
12.337×10^6	0.87 (±0.15)	0.59 (±0.07)	207.12 (±486.04)

The calculated metrics confirm that the proposed methodology gives satisfactory results in terms of accuracy, precision and timeliness despite the high uncertainty on the reinitialized values of the unknown loading inputs after load variation. Moreover, the obtained values show the usefulness of the timeliness metric. Indeed, we can see that the highest value of timeliness is at the prediction cycle $N_p = 12.337 \times 10^6$. This is explained by the fact that a significant part of the predicted RUL have fallen after the actual RUL value. Thus, even if the accuracy is the highest one, the timeliness value must be taken into account carefully to optimize maintenance decisions and avoid catastrophic events. As for the performance evaluation in the absence of the detection algorithm, the metrics could not even be calculated because the particle filter was not able to predict the acceleration of the crack growth and thus the threshold was never reached.

5. CONCLUSIONS

A model-based online prognosis method that is able to estimate and forecast unknown loading inputs was proposed in this paper. A particle filter was used for the joint input-state estimation and a two-sided CUSUM algorithm was integrated to detect load variations. Indeed, it was noticed that after an abrupt load variation, the particle filter had some difficulties to converge to the degradation state whose trajectory had suddenly changed. Therefore, the

role of the CUSUM algorithm is to monitor the unknown loading inputs values, and to give an alert when a load variation is detected. Once the particle filter has received this alert, the estimated values of the unknown loading inputs are reinitialized in an interval that is chosen from a priori knowledge. The association of these two algorithms has enabled to keep the RUL predictions accurate even after load variation.

The efficiency of the proposed methodology has been illustrated on real crack growth data from fatigue tests on composite materials. The performance evaluation metrics (accuracy, precision and timeliness) gave satisfactory results, and have demonstrated the ability of the method to deal not only with high nonlinearites but also with the various uncertainty sources that affect the prognosis process: modeling uncertainty, measurement uncertainty, external input uncertainty, and uncertainty related to the initial values of the unknown loading inputs. Finally, the proposed methodology has the advantage that it can be applied to various problems as long as an analytical model with unknown inputs is available. Even if simplifications have been realized on the model, as it was the case in this work, the algorithm is still able to adapt the estimation thanks to measurements from sensors.

In future work, the proposed prognosis method will be applied to fatigue crack growth data with more load variations. Moreover, other analytical models will be considered.

REFERENCES

Arulampalam, M.S., Maskell, S., Gordon, N., and Clapp, T. (2002). A tutorial on particle filters for online nonlinear/non-Gaussian Bayesian tracking. *IEEE Transactions on Signal Processing*, 50(2), 174–188.

Bakuckas, J. and Johnson, W.S. (1993). Application of fiber bridging models to fatigue crack growth in unidirectional titanium matrix composites. *Journal of Composites, Technology and Research*, 15(3), 242–255.

Baraldi, P., Mangili, F., and Zio, E. (2013). Investigation of uncertainty treatment capability of model-based and data-driven prognostic methods using simulated data. *Reliability Engineering and System Safety*, 112, 94–108.

Blanke, M., Kinnaert, M., Lunze, J., Staroswiecki, M., and Schröder, J. (2006). *Diagnosis and fault-tolerant control*, volume 691. Springer.

Bueckner, H. (1970). Novel principle for the computation of stress intensity factors. *Zeitschrift fuer Angewandte Mathematik & Mechanik*, 50(9).

Corbetta, M., Sbarufatti, C., Manes, A., and Giglio, M. (2015). Real-time prognosis of crack growth evolution using sequential monte carlo methods and statistical model parameters. *IEEE Transactions on Reliability*, 64(2), 736–753.

Daum, F. (2005). Nonlinear filters: beyond the Kalman filter. *Aerospace and Electronic Systems Magazine*, 20(8), 57–69.

Davidson, D. (1992). The micromechanics of fatigue crack growth at 25 c in ti-6al-4v reinforced with scs-6 fibers. *Metallurgical Transactions A*, 23(3), 865–879.

Ghosn, L.J., Kantzos, P., and Telesman, J. (1992). Modeling of crack bridging in a unidirectional metal matrix composite. *International Journal of Fracture*, 54(4), 345–357.

Gu, J., Barker, D., and Pecht, M. (2007). Uncertainty assessment of prognostics of electronics subject to random vibration. In *AAAI fall symposium on artificial intelligence for prognostics,Arlington, VA, USA*.

Johnson, W.S., Larsen, J.M., and Cox, B. (1996). *Life prediction methodology for titanium matrix composites*. 1253. ASTM International.

Laseure, N., Schepens, I., Micone, N., and De Waele, W. (2015). Effects of variable amplitude loading on fatigue life. *Sustainable Construction and Design*, 6(3).

Ling, Y. and Mahadevan, S. (2012). Integration of structural health monitoring and fatigue damage prognosis. *Mechanical Systems and Signal Processing*, 28, 89–104.

Maire, J., Levasseur, P., and Paulmier, P. (2000). Multiscale model of crack propagation in unidirectional metallic matrix composites. In *ECF13, San Sebastian 2000*.

McMeeking, R. and Evans, A. (1990). Matrix fatigue cracking in fiber composites. *Mechanics of Materials*, 9(3), 217–227.

Neerukatti, R.K., Liu, K.C., Kovvali, N., and Chattopadhyay, A. (2014). Fatigue life prediction using hybrid prognosis for structural health monitoring. *Journal of Aerospace Information Systems*, 11(4), 211–232.

Orchard, M., Kacprzynski, G., Goebel, K., Saha, B., and Vachtsevanos, G. (2008). Advances in uncertainty representation and management for particle filtering applied to prognostics. In *IEEE International Conference on Prognostics and Health Management, Denver, USA*.

Orchard, M.E. and Vachtsevanos, G.J. (2007). A particle filtering-based framework for real-time fault diagnosis and failure prognosis in a turbine engine. In *Mediterranean Conference on Control & Automation, MED'07*. IEEE.

Pais, M.J. and Kim, N.H. (2015). Predicting fatigue crack growth under variable amplitude loadings with usage monitoring data. *Advances in Mechanical Engineering*, 7(12), 1687814015619135.

Robinson, E., Marzat, J., and Raïssi, T. (2016). Model-based prognosis algorithms with uncertainty propagation: application to fatigue crack growth. In *3rd Conference on Control and Fault-Tolerant Systems (SysTol'16)*, 443–450. Barcelona, Spain.

Saha, B. and Goebel, K. (2008). Uncertainty management for diagnostics and prognostics of batteries using bayesian techniques. In *IEEE Aerospace Conference, Big Sky, MT, USA*, 1–8.

Tada, H., Paris, P.C., and Irwin, G.R. (1973). The stress analysis of cracks. *Handbook, Del Research Corporation*.

Tang, L., Kacprzynski, G.J., Goebel, K., and Vachtsevanos, G. (2009). Methodologies for uncertainty management in prognostics. In *Aerospace conference, 2009 IEEE*, 1–12. IEEE.

Zárate, B.A., Caicedo, J.M., Yu, J., and Ziehl, P. (2012). Bayesian model updating and prognosis of fatigue crack growth. *Engineering Structures*, 45, 53–61.

Zheng, D. and Ghonem, H. (1996). High temperature/high frequency fatigue crack growth in titanium metal matrix composites. In *Life prediction methodology for titanium matrix composites*. ASTM International.